*Journal of the Geological Society, London*, Vol. **162**, 2005, pp. 111–124. Printed in Great Britain.

# Subglacial meltwater channels and glaciofluvial deposits in the Kimberley Basin, Western Australia: 1.8 Ga low-latitude glaciation coeval with continental assembly

GEORGE E. WILLIAMS

*Geology and Geophysics, University of Adelaide, S.A. 5005, Australia (e-mail: george.williams@adelaide.edu.au)*

**Abstract:** A late Palaeoproterozoic unconformity surface developed on low-dipping sandstone in the Kimberley region, northwestern Australia, exhibits numerous linear, parallel grooves 10–50 mm deep, 40–80 mm wide and tens of metres long, and other erosional forms including sichelwannen. These features are interpreted as Nye channels and sculpted forms eroded by subglacial meltwaters. Sandstone-filled cracks exposed at the unconformity are viewed as periglacial frost fissures. An overlying conglomerate facies 1–15 m thick at the base of the *c*. 1800 Ma King Leopold Sandstone, Kimberley Basin succession, contains poorly sorted, pebble to boulder conglomerate and is interpreted as glaciofluvial in origin. The orientation of the Nye channels and sculpted forms and the palaeocurrent direction for the glaciofluvial deposits indicate westward ice flow. The conformably following, locally glauconitic quartzarenite of the King Leopold Sandstone probably accumulated in an epeiric sea, implying that glaciation reached close to sea level. Transgression in northwestern and central Australia at *c*. 1800 Ma may have been partly glacio-eustatic. Glaciation was initiated to the east of the Kimberley Basin, evidently in the Halls Creek Orogen, during a major phase of continental collision in Australia and worldwide supercontinental assembly. Recognition of the King Leopold glaciation, which occurred in low palaeolatitudes (<20°), shortens by 400 million years the claimed non-glacial interval between *c*. 2200 and 800 Ma.

**Keywords:** Western Australia, Palaeoproterozoic, Kimberley Basin, subglacial environment, glaciofluvial sedimentation.

A puzzling interval of *c*. 1400 million years with no verified glaciation occurs between early Palaeoproterozoic glaciations at 2400–2200 Ma in North America, South Africa, Scandinavia and Australia and the Neoproterozoic glaciations that affected all continents at 800–600 Ma (Eyles 1993; Crowell 1999). According to Eyles (1993), rifted, extensional tectonic settings provide conditions necessary for regional glaciation, and he ascribed the mid-Proterozoic non-glacial epoch in part to lessened global tectonic activity at that time. Another puzzling feature of the Proterozoic climatic record is the geological and palaeomagnetic evidence that some Proterozoic glaciations occurred near sea level in low palaeolatitudes (e.g. Schmidt & Williams 1995; Park 1997; Evans 2000).

As discussed here, the occurrence of a grooved sandstone surface and overlying poorly sorted conglomerate in the late Palaeoproterozoic Kimberley Basin, northwestern Australia, is relevant to these issues. The findings imply the presence of an ice cap near sea level in low palaeolatitudes on the North Australian Craton at a time of widespread orogeny and global supercontinental assembly, some 400 million years after the end of known early Palaeoproterozoic glaciations.

## Geological and palaeogeographical setting

A mostly undeformed, late Palaeoproterozoic succession unconformably overlies late Palaeoproterozoic (1890–1840 Ma) basement complexes in the Kimberley region, northwestern Australia (Griffin & Grey 1990*b*; Griffin *et al*. 1993; Thorne *et al*. 1999). The *c*. 1.8 Ga Kimberley Basin covers 160 000 km$^2$ and is the most extensive sedimentary basin in the region (Fig. 1). Sedimentary rocks of the underlying Speewah Basin (Sheppard *et al*. 1997) are exposed only on the upturned southeastern and southwestern margins of the Kimberley Basin. The main constituents of these two basins are the Speewah and Kimberley groups, respectively (Fig. 2), which together comprise up to 7 km of continental and shallow-marine siliciclastic sediments, dolomite and volcanic rocks that have fairly uniform lithologies and thicknesses over most of the outcrop areas.

Geological mapping in the southeastern Kimberley region originally placed the Luman Siltstone at the top of the Speewah Group, conformably followed by the 1200 m thick King Leopold Sandstone at the base of the Kimberley Group (Derrick *et al*. 1965; Gellatly *et al*. 1975). Later work in the Lansdowne–Mount Bedford area showed that a conglomerate facies within the King Leopold Sandstone rested on a very low-angle unconformity (Williams 1969). The unconformity is now known to be of regional extent, occurring to the west and NE of the Lansdowne–Mount Bedford area (Griffin *et al*. 1993; Sheppard *et al*. 1997; Thorne *et al*. 1999). The 500 m thick unit of quartzarenite and feldspathic sandstone lying between the Luman Siltstone and the unconformity is named the Bedford Sandstone and placed at the top of the Speewah Group (Williams 1969; Griffin *et al*. 1993; Sheppard *et al*. 1997; Thorne *et al*. 1999). The name King Leopold Sandstone is retained for the *c*. 700 m thick dominantly quartzarenite succession above the unconformity, which remains the lowermost formation of the Kimberley Group (Fig. 2).

The King Leopold Sandstone is overlain by tholeiitic basalts of the Carson Volcanics (270–700 m; Gellatly *et al*. 1975). Local pillow structures and associated sand waves, interpreted as subtidal, imply submarine extrusion (Plumb & Gemuts 1976). The Warton Sandstone (275–365 m) and the Pentecost Sandstone (*c*. 1000 m) comprise mature, quartzose and feldspathic sandstone (Gellatly *et al*. 1970, 1975). Rounded 1 mm grains of glauconite occur in the Pentecost Sandstone. The Elgee Siltstone (216 m) consists of massive red siltstone, sandstone and green mudstone. Plumb *et al*. (1990) envisaged the Kimberley Basin at

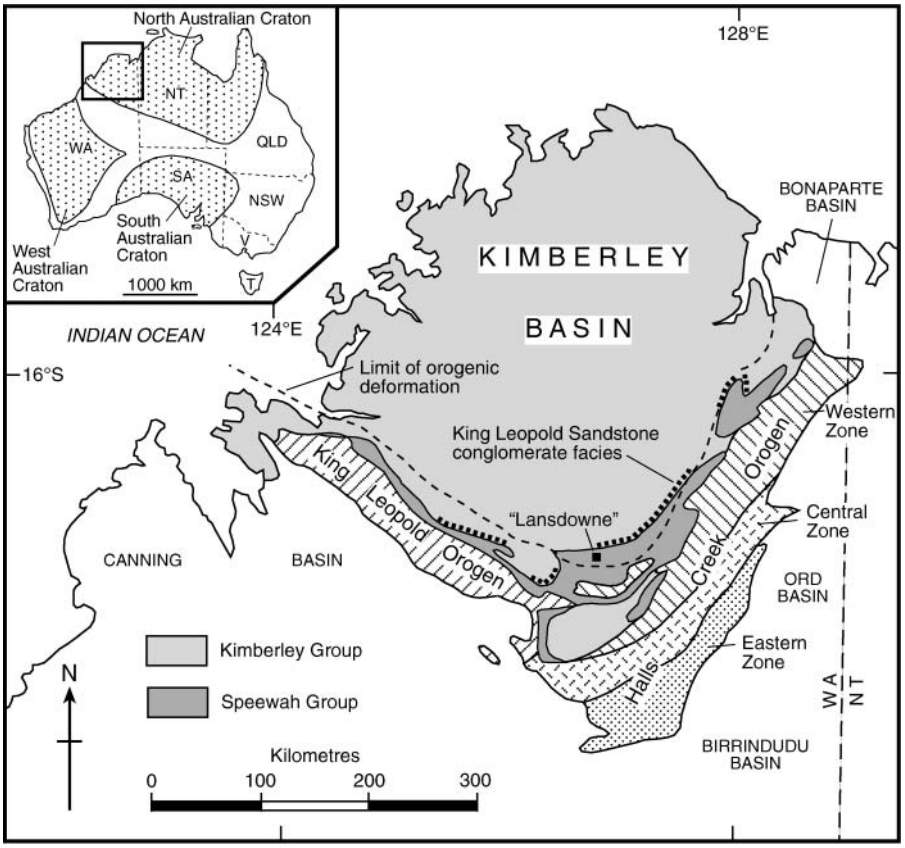


**Fig. 1.** Geological map showing the extent of the late Palaeoproterozoic Kimberley Group in the Kimberley Basin, the Speewah Group, and the King Leopold and Halls Creek orogens, northwestern Australia. Modified after Griffin & Grey (1990*b*), Tyler & Griffin (1990) and Sheppard *et al*. (1999). The bold dotted line marks the simplified line of outcrop of the conglomerate facies and correlative coarse-grained deposits at the base of the King Leopold Sandstone. The map of the main Precambrian cratons of Australia (inset) is modified after Myers *et al*. (1996).

the time of deposition as a broad, semi-enclosed shallow-marine basin similar to the North Sea. The Hart Dolerite intrudes the Speewah Group and lower Kimberley Group up to the Carson Volcanics, with which it may be coeval (McNaughton *et al*. 1999). The Kimberley Group is unconformably overlain by late Neoproterozoic glaciogenic rocks in the southern and eastern parts of the basin.

A maximum age for the Kimberley Group is provided by a U–Pb zircon age of $1834 \pm 3$ Ma for felsic volcanic rocks interbedded with sediments of the Valentine Siltstone in the Speewah Group (Page & Sun 1994) and a minimum age by U–Pb ages of $1704 \pm 7$ and $1704 \pm 14$ Ma for diagenetic xenotime from the Warton Sandstone and Pentecost Sandstone, respectively (McNaughton *et al*. 1999). A Rb–Sr whole-rock age of 1807 Ma for the Carson Volcanics (Bennett *et al*. 1975) and a U–Pb zircon age of $1790 \pm 4$ Ma for the Hart Dolerite that is interpreted as the age of igneous crystallization (Ozchron 2004) imply that the King Leopold Sandstone was deposited either near 1800 Ma or a little earlier. The unconformably underlying Bedford Sandstone was deposited around 1820 Ma.

Palaeomagnetic data for the Kimberley Group are confined to the Elgee Siltstone (Li 2000), whose red siltstone and mudstone contain an extremely stable remanence carried by hematite (declination $D = 92.2°$, inclination $I = 14.9°$, $\alpha_{95} = 6.4°$). Li (2000) interpreted the remanence to be primary, which implies that the Elgee Siltstone was deposited in low palaeolatitudes (7.6 $+3.4/-3.3°$). McElhinny & Evans (1976) studied the palaeomagnetism of the Hart Dolerite in the southern Halls Creek Orogen. After magnetic cleaning, samples from 12 sites gave a mean direction (corrected for dip of nearby sedimentary rocks) of $D = 121°$, $I = 2°$, $\alpha_{95} = 31$) and yielded a positive baked contact test. McElhinny & Evans (1976) regarded the remanence as primary, indicating a palaeolatitude $1 \pm 17°$ for intrusion. These data and the apparent polar wander path for the Australian Precambrian (Schmidt & Clark 1994; Idnurm *et al*. 1995; Li 2000; Williams *et al*. 2004) are consistent with low palaeolatitudes ($<20°$) for northwestern Australia at 1.8 Ga.

Most of the Kimberley Group is undeformed and a broad dissected plateau is developed on the flat-lying rocks. Near the margins of the Kimberley Basin the succession is folded and faulted and is included in the Halls Creek Orogen to the SE and the King Leopold Orogen to the SW (Fig. 1; Griffin & Grey 1990*a*). The Halls Creek Orogeny at 1830–1800 Ma represents the final suturing of the Kimberley Craton onto the North Australian Craton to the SE (Tyler & Page 1996).

## Sedimentary succession in the Lansdowne–Mount Bedford area

The Bedford Sandstone and King Leopold Sandstone in the Lansdowne–Mount Bedford area (inset, Fig. 3) constitute a laterally persistent succession that dips 5–15° northward and crops out boldly to form the King Leopold Ranges, which attain an elevation of 800 m. The stratigraphy, characteristics and depositional environments of these mostly arenaceous formations are summarized in Table 1. Importantly, the formations are separated by a very low-angle unconformity that is overlain by a thin, widespread conglomerate facies at the base of the King Leopold Sandstone (Fig. 3).

Helicopter transport to much of the area was required because of the rugged terrain. Most of the data came from detailed studies and traverses centred on 18 evenly spaced sites between Mount Bedford and Lansdowne. Ten representative sites are shown in Figure 3.

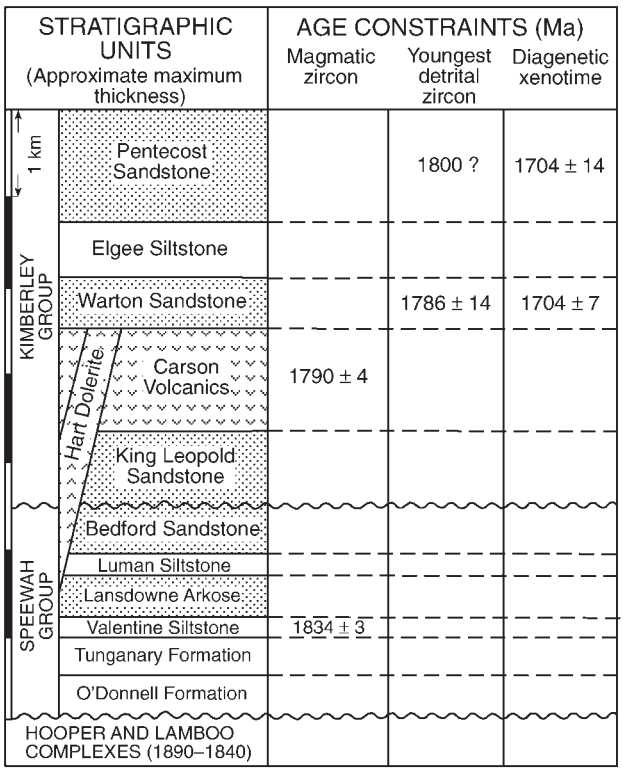


**Fig. 2.** Generalized stratigraphic column for the Speewah and Kimberley groups, with available ages (in Ma). Modified after McNaughton *et al*. (1999). The age of the Hooper and Lamboo basement complexes in the King Leopold and Halls Creek orogens is from Griffin *et al*. (1993) and Thorne *et al*. (1999).

### *Bedford Sandstone*

The lowest 100 m of the Bedford Sandstone comprise white to pale red, medium- to coarse-grained, well-sorted quartzarenite (Wentworth grade scale terminology). Grains are subrounded to well rounded, with quartz-cement overgrowths. Trough and tabular cross-bedding is common, with most trough cross-bed sets being 0.15–0.3 m thick and tabular cross-bed sets up to 0.6 m thick. The orientation of trough axes indicates southward flow.

The succeeding 400 m thick succession commences with numerous bands of granule sandstone and pebble conglomerate up to 50 mm thick, followed by pale red, poorly sorted, medium- to very coarse-grained and locally pebbly feldspathic sandstone. Grains are subangular to rounded, with a sericitic matrix containing ultra-fine (≤1 μm) hematitic pigment. Mudstone rip-up conglomerate occurs locally, although mudstone interbeds were not observed. Trough cross-bedding is common and predominates over tabular cross-bedding. Most trough cross-bed sets are 0.15–0.4 m thick and tabular cross-bed sets are up to 1 m thick. One trough form seen in plan is 8 m wide and 0.75 m deep and extends east–west for more than 20 m. Pebbles are mostly of quartz and also of quartzite and sandstone. Palaeocurrent directions (Fig. 4a), representing the azimuths of trough axes seen on low-dipping beds, are strongly unimodal and indicate west-southwestward flow (vector mean 254°, vector magnitude 95.4%; method of calculation from Potter & Pettijohn (1977)).

### *Unconformity surface on the Bedford Sandstone*

A generally planar, very low-angle unconformity occurs between the Bedford Sandstone and the King Leopold Sandstone. The unconformity roughly parallels the major bedding planes in the Bedford Sandstone, although field observations and data from

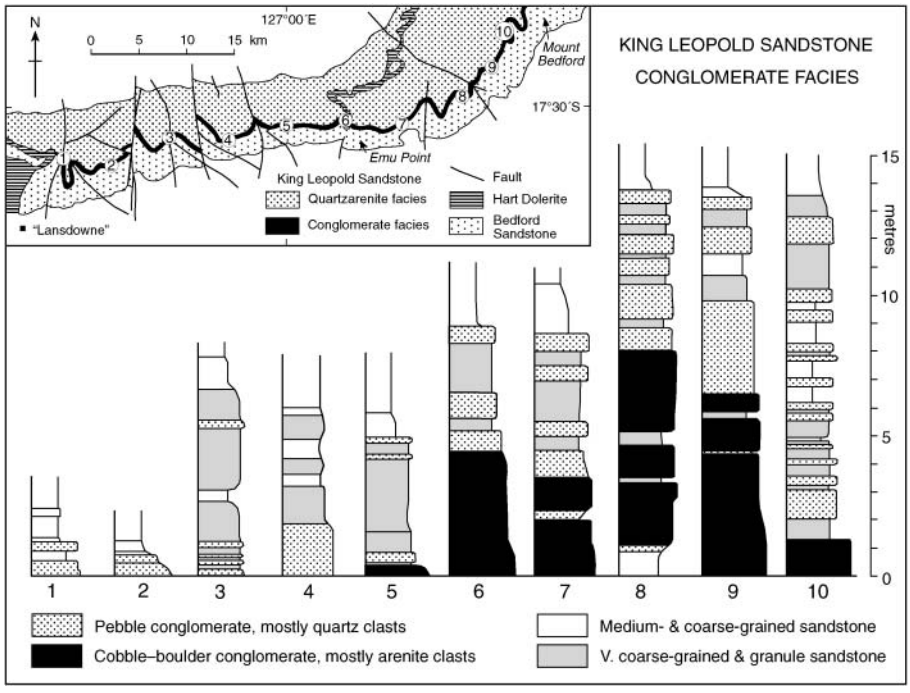


**Fig. 3.** Graphic logs of the conglomerate facies at the base of King Leopold Sandstone between Lansdowne and Mount Bedford. The conglomerate facies unconformably overlies the Bedford Sandstone, the top of which is taken to be coplanar. Wentworth grade scale terminology used. The inset shows the localities of the measured sections for the graphic logs (geological sketch map modified from Derrick *et al*. (1965)).

**Table 1.** *Stratigraphy, characteristics and interpreted palaeoenvironments of the Bedford Sandstone and King Leopold Sandstone (late Palaeoproterozoic) in the Lansdowne–Mount Bedford area, southeastern Kimberley region, Western Australia*

| Formation | Characteristics | Thickness (m) | Mean palaeocurrent direction | Palaeoenvironment |
|---|---|---|---|---|
| King Leopold Sandstone | *Quartzarenite facies*<br>White to pale grey, texturally mature, fine- to coarse-grained quartzarenite. Local pebble bands. Scattered grains of glauconite. Trough cross-bedding (sets 0.15–0.4 m thick) and tabular cross-bedding (sets ≤2 m thick). Symmetrical ripple marks. Polygonal mudstone rip-up conglomerate | 250 | To the south. Locally to the NW | Shallow epeiric sea with directional currents |
| | Pale purple to pale grey, flaggy, fine-grained quartzarenite. Silty bands. Flat-bedding with primary current lineation. Ripple marks. Rare trough and tabular cross-bedding | 60 | To the south | Shallow epeiric sea with directional currents |
| | White to pale pink, texturally mature, medium- to coarse-grained quartzarenite. Local pebble bands. Trough cross-bedding (sets 0.15–0.4 m thick) and tabular cross-bedding (sets ⩽2 m thick). Flat-bedding near top of unit. Ripple marks. Polygonal mudstone rip-up conglomerate. Lenticular facies (0–20 m thick) of greyish purple mudstone and fine-grained sandstone with flute casts, near base of unit | 350–370 | To the south | Shallow epeiric sea with directional currents. Transgressive |
| | *Conglomerate facies*<br>Poorly sorted cobble and boulder conglomerate, matrix- and clast-supported, local imbrication; clasts of quartzarenite and sandstone, subrounded to well rounded, rarely striated. Poorly sorted quartz-pebble conglomerate and medium-grained to granule sandstone. Trough cross-bedding (sets 0.15–0.3 m thick). Rare ventifacts. Sandstone-filled vertical cracks in the Bedford Sandstone | 1–15 | To the west | Glaciofluvial deposition. Subsequent periglacial setting, with frost fissures and strong winds |
| | Linear grooves and other erosional features exhibited by the unconformity surface developed on the Bedford Sandstone | | | Nye channels and sculpted forms cut by subglacial meltwaters |
| | VERY LOW-ANGLE UNCONFORMITY | | | |
| Bedford Sandstone | Pale red, texturally immature, medium- to very coarse-grained, locally pebbly feldspathic sandstone with sericitic–hematitic matrix. Trough cross-bedding (sets 0.15–0.4 m thick) and tabular cross-bedding (sets ⩽1 m thick). Mudstone rip-up conglomerate. Bands of granule sandstone and pebble conglomerate | 400 | To the WSW | Braided-river deposition. Regressive |
| | White to pale red, texturally mature, medium- to coarse-grained quartzarenite. Trough cross-bedding (sets 0.15–0.3 m thick) and tabular cross-bedding (sets ⩽0.6 m thick). Flat-bedding with primary current lineation | 100 | To the south | Shallow epeiric sea with directional currents |

mineral-exploration drilling show that the Bedford Sandstone has a slightly steeper (1–2°) northward dip than the King Leopold Sandstone. The unconformity shows microrelief of 1–10 m in several places, where depressions and apparent channels bounded by vertical joints in the Bedford Sandstone are filled with conglomerate at the base of the King Leopold Sandstone. These and other erosional features, discussed below, indicate that the Bedford Sandstone was at least moderately lithified prior to deposition of the King Leopold Sandstone.

*Linear grooves.* Near Lansdowne (17°33′S, 126°47′E), the recently exhumed unconformity surface developed on the Bedford Sandstone exhibits numerous linear, parallel grooves 10–50 mm deep, 40–80 mm wide and spaced 60–350 mm apart (Figs 5 and 6). Typically the grooves are rounded in cross-section. The grooves trend east–west (100°–280°) for up to tens of metres within the limits of local exposure (Fig. 5). Similarly oriented grooves are exposed discontinuously over an east–west distance of 1 km. Where the surface of the Bedford Sandstone is partly exhumed, grooves are filled with pebbly sandstone of the basal King Leopold Sandstone (Fig. 6a), indicating that the grooves were cut in the Bedford Sandstone prior to its burial. The grooves commonly cut across the traces of cross-strata in the Bedford Sandstone shown at the unconformity surface (Figs 5 and 6b) and are unrelated to joints in the Bedford Sandstone (Fig. 6c). Some grooves deepen and terminate fairly abruptly (Fig. 6c). In several places, flat-bottomed grooves 100–300 mm wide are separated by narrow ridges 10–30 mm high (Fig. 6d).

*Other erosional features.* The unconformity surface exhibits a variety of other erosional features. Parts of the surface are smoothed, with only traces of the grooves being discernible (Fig. 7a). The surface also shows crescent-shaped hollows termed ‘sichelwannen’ (Fig. 7b) and cross-strata in the Bedford Sandstone that have been etched and undercut (Fig. 7c). Locally, linear grooves have been delicately eroded to form small meanders with undercut walls (Fig. 7d). Some grooves are deepened, widened and slightly sinuous (Fig. 7e), causing adjacent grooves to converge and join at acute angles in places; usually the junction points to the west. Other features include ridges 50–100 mm wide that parallel the grooves and have rounded terminations to the east (Fig. 7f), and rare potholes up to 0.5 m

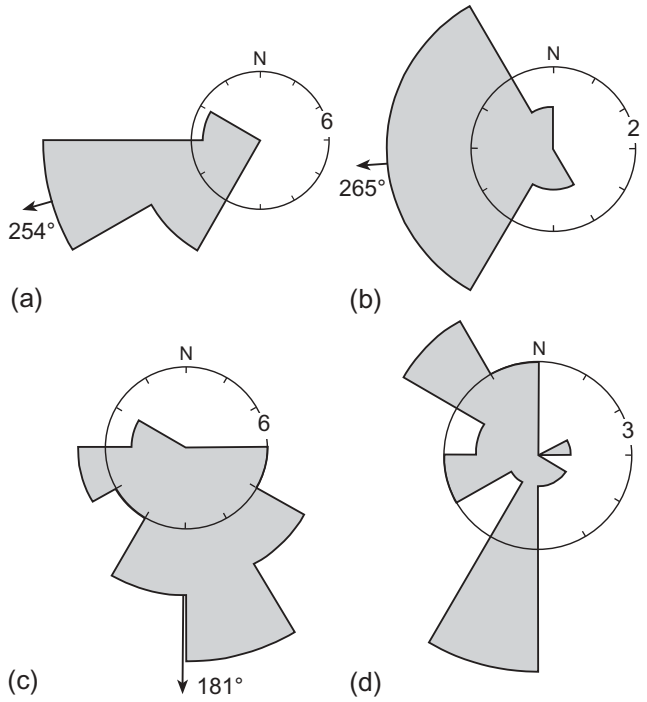


**Fig. 4.** Rose diagrams of palaeocurrent data for azimuths of troughs measured on low-dipping sandstone beds in the Lansdowne–Mount Bedford area. Class interval 30°. (**a**) Bedford Sandstone, upper 400 m (vector mean 254°, vector magnitude 95.4%, $n = 35$). (**b**) King Leopold Sandstone, conglomerate facies (vector mean 265°, vector magnitude 76.7%, $n = 19$). (**c**) King Leopold Sandstone, lower quartzarenite facies (vector mean 181°, vector magnitude 69.1%, $n = 59$). (**d**) King Leopold Sandstone, upper quartzarenite facies ($n = 24$).

across and 0.3 m deep.

The orientation of sichelwannen, the manner of local undercutting, and the convergence of some grooves are consistent with erosion of the sandstone surface by currents flowing to the west along the line of the grooves.

*Sandstone-filled vertical cracks.* Vertical cracks up to 50 mm wide in the Bedford Sandstone exposed at the unconformity are filled by dykes of pebbly sandstone (Fig. 8). The maximum depth of such cracks cannot be determined but some are >200 mm deep. One dyke in the Bedford Sandstone extends upwards into overlying pebbly sandstone of the conglomerate facies. The corners where the cracks intersect the unconformity surface are sharp and show no sign of erosion (Fig. 8a). In plan, the sandstone-filled cracks intersect in places (Fig. 8b) and outline irregular polygons several metres across. The orientation of all filled cracks seen on the unconformity surface near Lansdowne (Fig. 9) shows a conjugate pattern that is unrelated to the trend of the grooves.

## *King Leopold Sandstone*

*Conglomerate facies.* Graphic logs of the conglomerate facies that unconformably overlies the Bedford Sandstone are shown in Figure 3. This facies occurs continuously over 55 km between Lansdowne and Mount Bedford and has been traced for 30 km to the NE in the Durack Range (Derrick *et al*. 1965). Pebble–boulder conglomerates at the base of the King Leopold Sandstone further to the NE in the Mount Remarkable and Lissadell areas (Plumb 1968; Carter 1976; Sheppard *et al*. 1997) and granule sandstone with scattered pebbles at the base of the King Leopold Sandstone in the Lennard River area to the west (Griffin *et al*. 1993) are correlative with the conglomerate facies in the Lansdowne–Mount Bedford area. A strike length of >300 km therefore is indicated for this coarse-grained facies (Fig. 1).

The conglomerate facies in the area studied is 1–15 m thick, being thickest and coarsest in the east between Emu Point and Mount Bedford. There it is characterized by tabular, ungraded beds 0.5–4.5 m thick of poorly sorted, bimodal to polymodal, cobble and boulder conglomerate (Fig. 10a and b), and interbeds <1 m thick of poorly sorted, coarse-grained to granule sandstone and pebble conglomerate. Contacts between beds typically are sharp. The cobble and boulder conglomerate comprises clasts of quartzarenite and sandstone, some quartz-veined, up to 1 m in diameter and a matrix of coarse-grained to granule sandstone. The clasts are commonly matrix-supported, and clast-supported and locally imbricate conglomerate also is present. East–west-

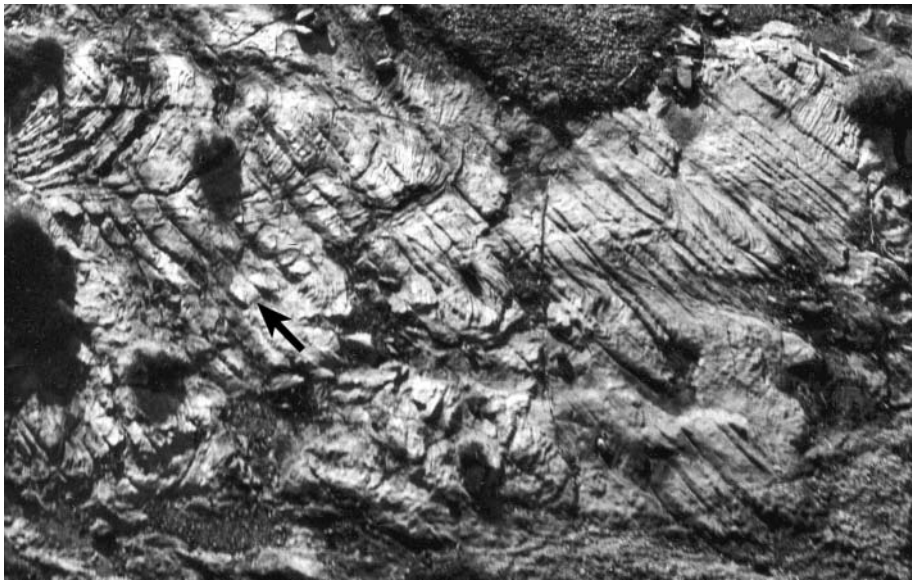

**Fig. 5.** Unconformity surface developed on the low-dipping Bedford Sandstone near Lansdowne, as viewed from a helicopter. The area covered by the photograph measures *c*. 10.5 m × 6.5 m; NW to top of photograph. The east–west-trending grooves cut across the arcuate traces of trough cross-bedding in the Bedford Sandstone, in the upper left. The arrow shows the palaeocurrent direction for the overlying conglomerate facies of the King Leopold Sandstone and the inferred direction of ice flow.

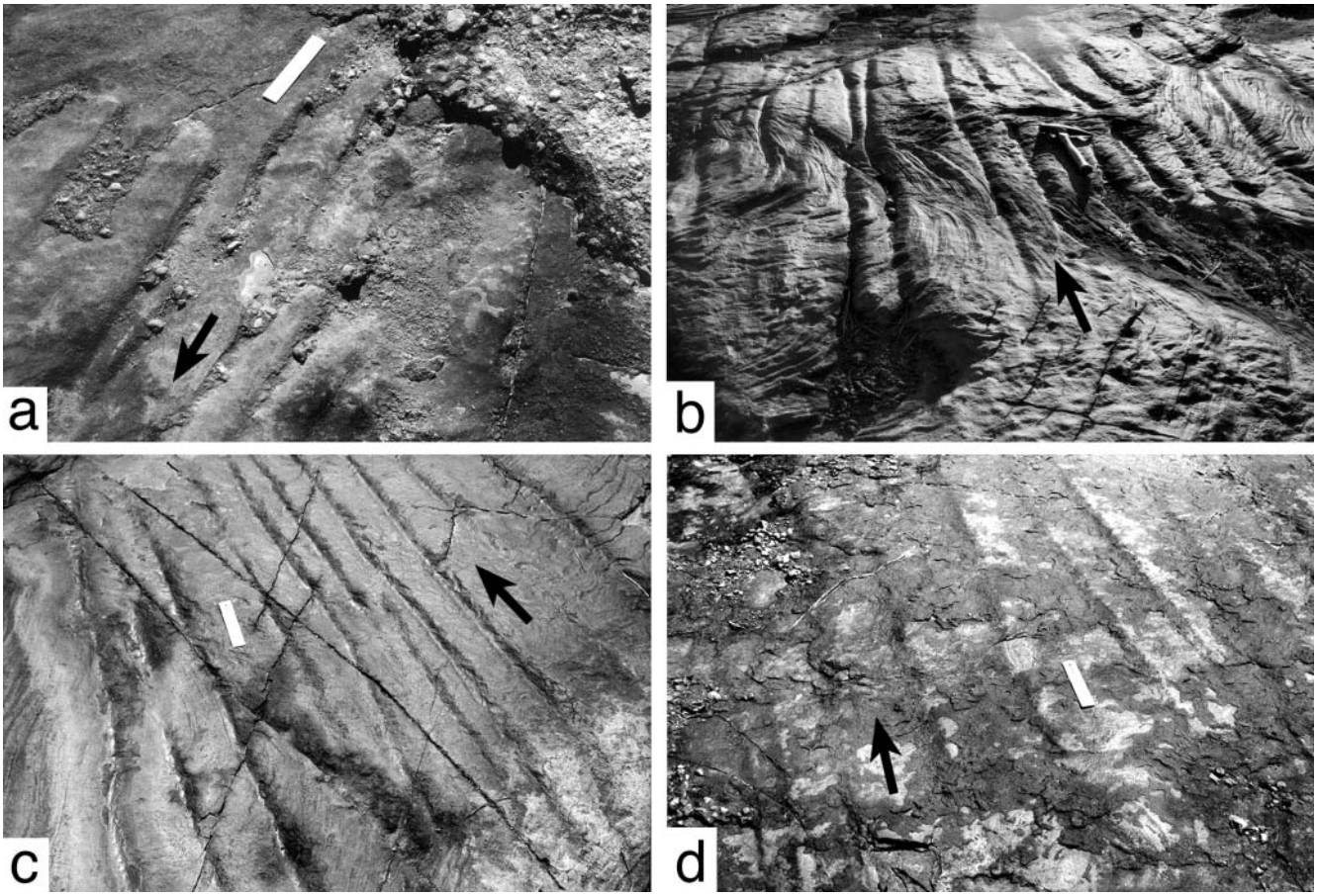


**Fig. 6.** Grooves in the unconformity surface of the Bedford Sandstone near Lansdowne. The arrows show the palaeocurrent direction for the overlying conglomerate facies of the King Leopold Sandstone and the inferred direction of ice flow. (**a**) Grooves partly filled with pebbly sandstone and covered by pebble conglomerate in the top right. NE to top of photograph. Scale 150 mm. (**b**) Near-linear grooves cutting across the curved traces of trough cross-bedding in the Bedford Sandstone. View looking west. Hammer for scale. (**c**) Linear, parallel grooves, some of which deepen and terminate fairly abruptly (to right of scale). The joints in the Bedford Sandstone are unrelated to the grooves. WNW to top of photograph. Scale 150 mm. (**d**) Broad, flat-bottomed grooves separated by narrow ridges 10–30 mm high. WNW to top of photograph. Scale 150 mm.

trending clusters of boulders ⩽1 m high and up to 5 m long (Fig. 10c) occur in places. Clasts are subrounded to well rounded (estimated visually using the roundness grades of Pettijohn (1975)). Clasts with flatiron shapes and rare striations (Fig. 10d) also are present. The interbeds of pebble conglomerate contain clasts of vein quartz, metaquartzite, mylonite, conglomeratic sandstone, chert and jasper. A grab sample of 100 pebbles near Mount Bedford contained 59 of quartzarenite and sandstone, 23 of vein quartz, 16 of quartzose cataclasite, and two of metaquartzite.

The cobble and boulder conglomerate is overlain and replaced laterally by poorly sorted, coarse-grained to granule sandstone and pebble conglomerate that lie directly on the Bedford Sandstone near Lansdowne in the western part of the study area. Beds are 0.15–0.4 m thick and usually more pebbly at the base. The pebbles are subangular to subrounded and consist mostly of quartz; a grab sample of 100 pebbles near Lansdowne contained 80 of vein quartz, 12 of quartzarenite, four of cataclasite, two of sandstone, one of metaquartzite, and one of chert. Trough cross-bedding in the sandstone (sets 0.15–0.3 m thick) indicates overall westward flow of palaeocurrents (trough azimuth vector mean 265°, vector magnitude 76.7%; Fig. 4b). It is noteworthy that the palaeocurrent direction parallels the line of the grooves in the underlying unconformity surface of the Bedford Sandstone.

The conglomerate facies contains rare pebbles and cobbles of quartzarenite, quartzite, quartz and chert displaying sharp edges, flutes and pits. These features are typical of ventifacts. Of 22 such clasts observed near Mount Bedford, Emu Point and Lansdowne, 13 (59%) are classifiable as einkanter (Fig. 10e) and have a mean clast length of 123 mm, four (18%) are dreikanter (mean clast length 51 mm), and five (23%) with flutes and pits are tafoni (Fig. 10f) (mean clast length 70 mm).

The pebble conglomerate is moderately to strongly radioactive resulting from the presence of detrital thorium heavy minerals, mainly thorogummite, florencite, thorite and cheralite, and has been explored for possible uranium mineralization (Hughes & Harms 1975; Carter 1976).

*Quartzarenite facies.* A succession *c*. 700 m thick comprising mostly white and also pale grey, pale pink and pale purple, well-sorted, fine-, medium- and coarse-grained quartzarenite conformably overlies the conglomerate facies. Grains are mostly rounded to well rounded, with quartz-cement overgrowths. Scattered, rounded grains of glauconite 0.5–1.0 mm in diameter occur in quartzarenite in the upper part of the succession.

Most of this arenaceous succession displays abundant trough and tabular cross-bedding. Trough cross-bed sets typically are 0.15–0.4 m thick and tabular cross-bed sets are up to 2 m in

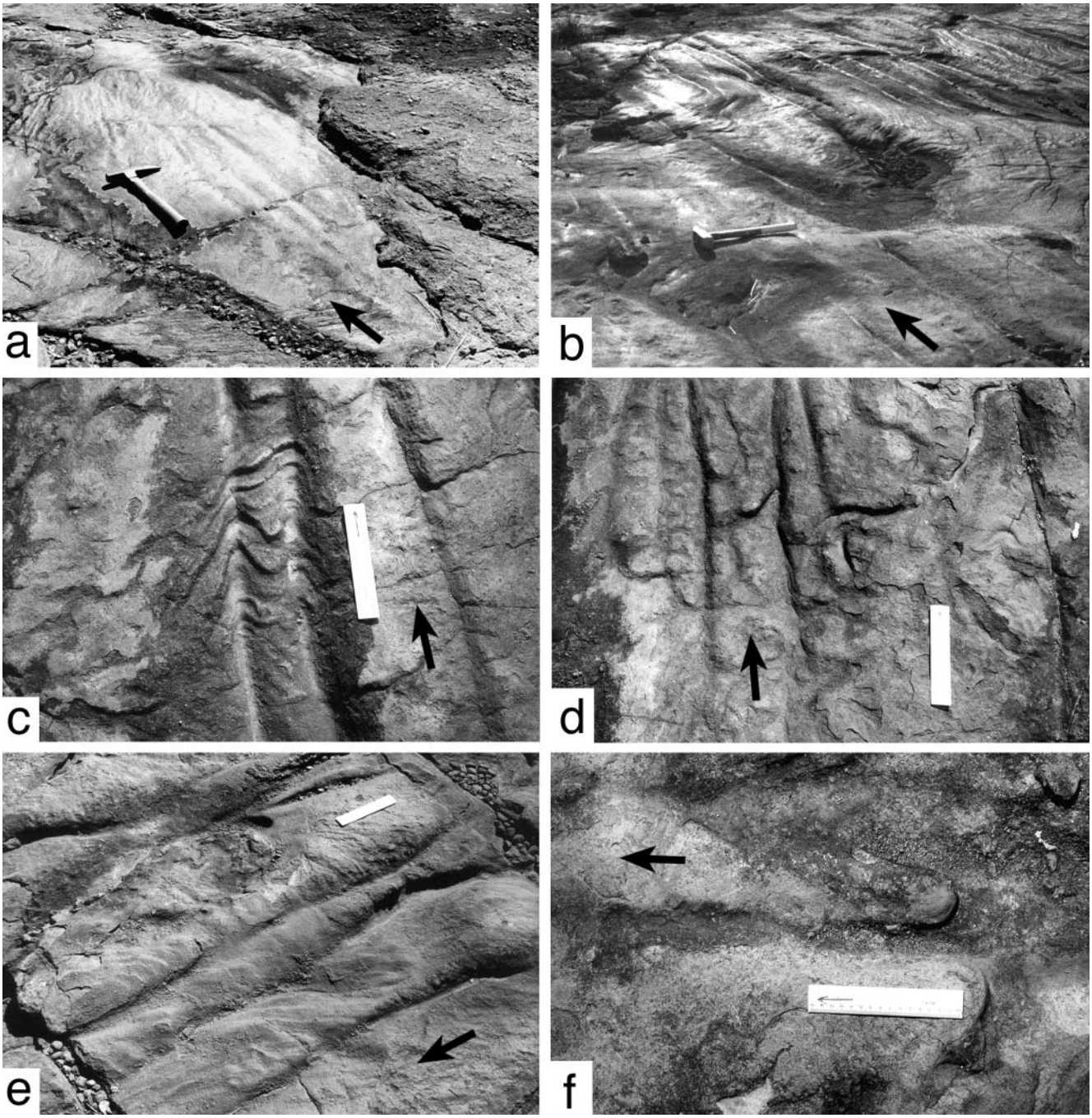


**Fig. 7.** Sculpted forms exhibited by the unconformity surface of the Bedford Sandstone near Lansdowne. The arrows show the palaeocurrent direction for the overlying conglomerate facies of the King Leopold Sandstone and the inferred direction of ice flow. (**a**) Smoothed surface, with only traces of grooves being discernible. A vertical crack in the Bedford Sandstone (near hammer handle) is filled with pebbly sandstone derived from the conglomerate facies, which buries the unconformity surface to the right. View looking NW. Hammer 350 mm long. (**b**) Crescent-shaped hollow (sichelwanne) to the right of the hammer. View looking NW. Hammer 300 mm long. (**c**) Etched and undercut cross-strata in the Bedford Sandstone. West to top of photograph. Scale 150 mm. (**d**) Linear grooves that have been delicately eroded to form small meanders with undercut walls. West to top of photograph. Scale 150 mm. (**e**) Deepened, widened and slightly sinuous grooves. NNE to top of photograph. Scale 150 mm. (**f**) Ridges that are parallel to the grooves and have rounded terminations to the east. North to top of photograph. Scale 150 mm.

thickness, with cross-strata locally overturned downcurrent. Small-scale ripple marks, commonly straight symmetrical, occur throughout the succession. Local mudstone rip-up conglomerate contains numerous polygonal plate-like clasts. A restricted facies 0–20 m thick that occurs 5–15 m above the unconformity west of Emu Point comprises greyish purple mudstone and fine-grained sandstone displaying ripple-drift cross-lamination and flute casts.

Trough-axis azimuths of cross-bed sets indicate dominant southward flow of palaeocurrents (vector mean 181°, vector magnitude 69.1%; Fig. 4c). Bimodal palaeocurrent directions occur near the top of the succession (Fig. 4d), with north-

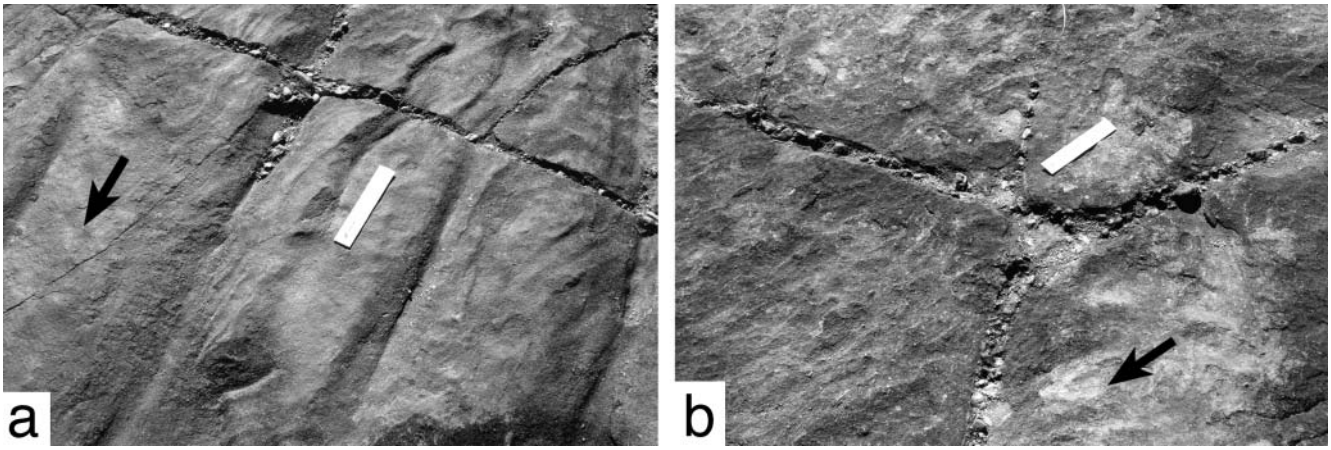


**Fig. 8.** Vertical cracks seen at the unconformity surface of the Bedford Sandstone near Lansdowne. The arrows show the palaeocurrent direction for the overlying conglomerate facies of the King Leopold Sandstone and the inferred direction of ice flow. (**a**) Plan view of a crack with sharp corners that is filled with pebbly sandstone. ENE to top of photograph. Scale 150 mm. (**b**) Plan view of intersecting cracks in the Bedford Sandstone that are filled with pebbly sandstone. NE to top of photograph. Scale 150 mm.

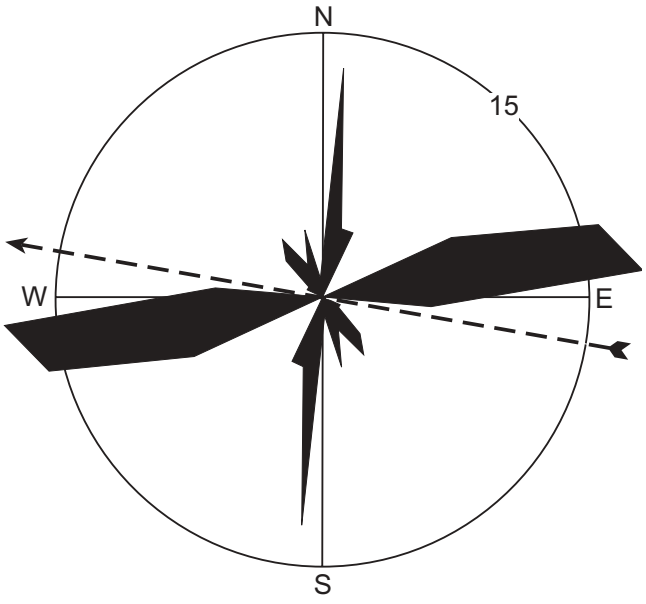


**Fig. 9.** Rose diagram of the orientations of all sandstone-filled vertical cracks seen at the unconformity surface of Bedford Sandstone near Lansdowne (number of measurements 86). The dashed line shows the orientation of grooves in the unconformity surface and the arrow the inferred direction of ice flow.

westward flow marked by an influx of granules and small pebbles.

## Deposition of the sandstone and quartzarenite facies

A variety of sedimentological criteria, including petrography, texture, lithology and sedimentary structures, must be applied in the environmental analysis of Precambrian arenites (Blake *et al*. 1987; Abbott & Sweet 2000). The quartzarenites of the King Leopold Sandstone and the lowest 100 m of the Bedford Sandstone are characterized by textural and mineralogical maturity and medium-scale tabular and trough cross-bedding yielding polymodal palaeocurrent directions. Features displayed by the King Leopold Sandstone (Table 1) include wave-generated symmetrical ripple marks, polygonal plate-like intraclasts of mudstone suggesting the erosion of desiccated mudflats, local mudstone–sandstone facies with flute casts, and rounded grains of glauconite. The predominantly southward palaeocurrent directions for all the quartzarenite units agree with the southward to southeastward regional palaeocurrent directions determined for the King Leopold Sandstone, Warton Sandstone and Pentecost Sandstone over 150 000 km$^2$ throughout the Kimberley Basin (Gellatly *et al*. 1970). As noted above, rounded grains of glauconite also occur in the Pentecost Sandstone. These features accord with shallow-marine settings (Plumb *et al*. 1990; Abbott & Sweet 2000) and point to deposition of the quartzarenites of the King Leopold Sandstone and Bedford Sandstone in shallow epeiric seas marked by directional currents (Eriksson *et al*. 1998).

In contrast, the features characterizing the upper 400 m of the Bedford Sandstone, namely textural and mineralogical immaturity, locally pebbly nature, abundant trough cross-bedding yielding strongly unimodal palaeocurrent data, tabular cross-bedding, and lack of mudstone interbeds together are consistent with the deposits of sand-bed rivers, particularly braided rivers of Platte type (Miall 1996). Palaeocurrent data indicate an eastern provenance.

It is concluded that shallow-marine deposition in the southeastern Kimberley region was interrupted *c*. 1820 Ma by an influx of braided-river deposits that indicate an elevated source area to the east. A relative fall in sea level at that time is implied.

## Origin of the grooved surface and conglomerate facies

### *Subglacial meltwater channels (Nye channels)*

The linear grooves in the unconformity surface developed on the Bedford Sandstone cannot be ascribed to erosion by free-flowing streams, because dendritic and anastomosing drainage patterns are absent. The manner in which the grooves extend across irregularities such as cross-bedding in the Bedford Sandstone also argues against normal stream erosion. Slip planes resulting from Basin and Range detachment faulting in Arizona, USA, exhibit grooves and ridges bearing some similarity to those

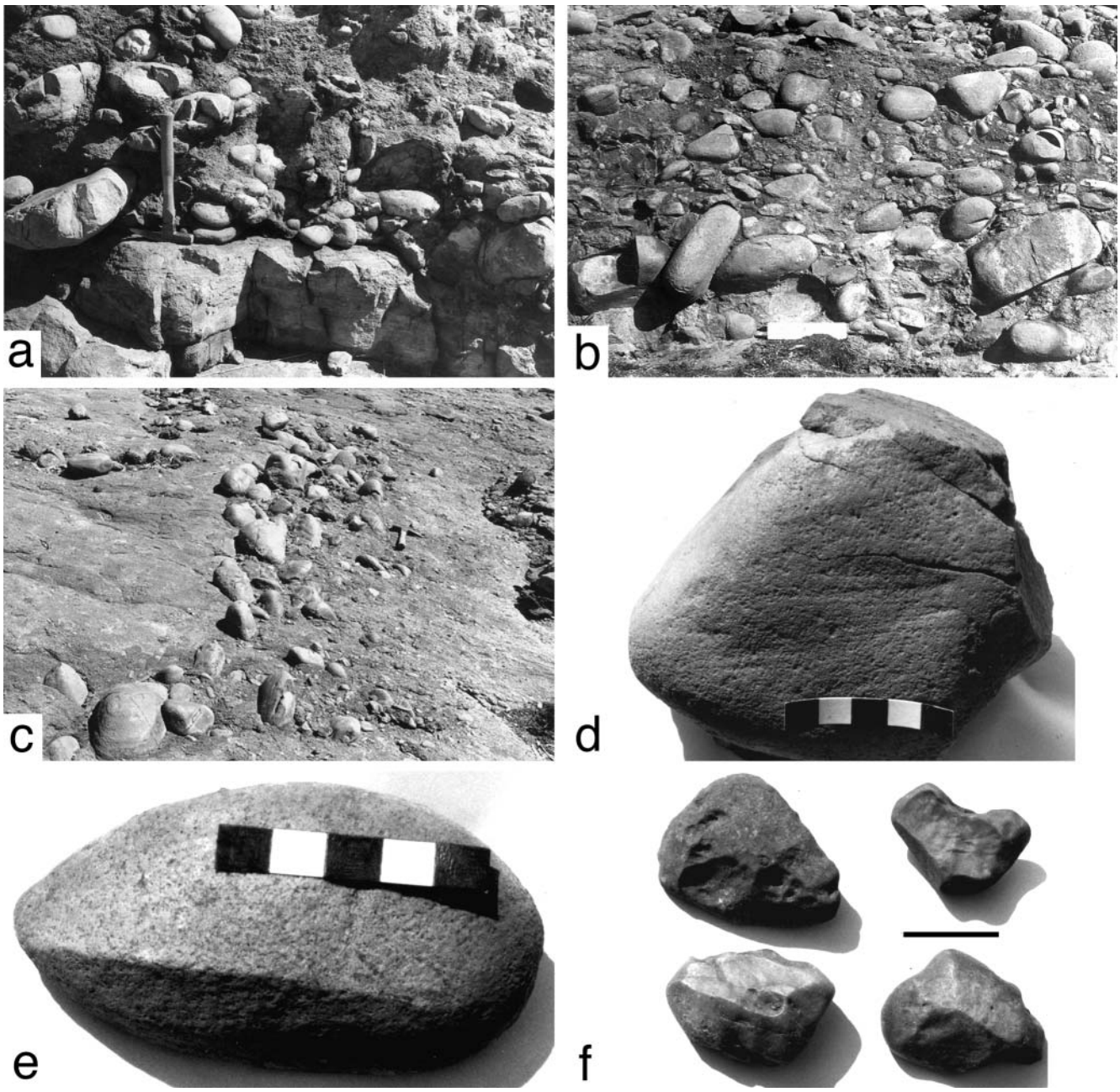


**Fig. 10.** (**a**) Matrix-supported boulder conglomerate at the base of the conglomerate facies of the King Leopold Sandstone, resting unconformably on the Bedford Sandstone near Emu Point. View looking west. Hammer 350 mm long. (**b**) Vertical section of matrix- and clast-supported boulder conglomerate with imbricate clasts, near the base of the conglomerate facies SW of Mount Bedford (Fig. 3, graphic log 9). View looking west. Scale 150 mm. (**c**) Cluster of boulders exposed on the surface of a bed of pebbly sandstone in the conglomerate facies near Emu Point. View looking west. Hammer for scale. (**d**) Striated cobble of sandstone from the conglomerate facies near Emu Point. Scale 50 mm. (**e**) Quartzite einkanter from the conglomerate facies near Mount Bedford. Scale 50 mm. (**f**) Quartz ventifacts with facets, flutes and pits, from the conglomerate facies near Lansdowne. Scale bar 30 mm.

formed at the base of 'soft-bedded' glaciers (Eyles & Boyce 1998), but these faults are steeply dipping (80°) and cannot be compared to the very low angle (1–2°) unconformity surface of wide extent below the King Leopold Sandstone. Moreover, the grooves in the unconformity surface are unrelated to joints in the Bedford Sandstone. Hence tectonic processes cannot account for the grooves.

The grooves in the Bedford Sandstone have many features in common with Nye channels, which are subglacial meltwater channels cut into bedrock or cemented rock (Walder & Hallet 1979; Moncrieff & Hambrey 1988; Sharp *et al*. 1989; Benn & Evans 1998; Gray 2001). Such channels can carry large volumes of sediment-laden meltwater that can be a potent agent of erosion. Most Nye channels are less than a metre to a few tens of metres wide. Dendritic and anastomosing drainage patterns are displayed but, importantly, some Nye channels either are linear or of low sinuosity (Walder & Hallet 1979; Sharp *et al*. 1989; Gray 2001). Many Nye channels have abrupt terminations and unlinked segments (Moncrieff & Hambrey 1988; Sharp *et al*. 1989; Benn & Evans 1998). Linear subparallel grooves 50–

100 mm deep, 80–200 mm wide and with rounded cross-sections are cut in a flat-topped exposure of Pennsylvanian sandstone *c*. 100 m × 100 m in extent in Indiana, USA (Gray 2001). The grooves exhibit small erosional features including undercut walls, small-amplitude meanders, divergence around obstacles such as concretions, and rare branching and rejoining at acute angles. Gray (2001) interpreted the grooves as small Nye channels that were produced by subglacial meltwaters near the southern limit of pre-Wisconsinan glacial deposits in Indiana. These grooves are closely comparable with the grooves in the Bedford Sandstone, which also qualify as Nye channels.

Nye channels tend to parallel glacier flowlines (Walder & Hallet 1979; Sharp *et al*. 1989; Benn & Evans 1998) and commonly are termed 'ice-directed channels'. The linearity of some Nye channels has led to the suggestion that they were initiated along abrasional features such as striations and gouges cut by a flowing glacier (Walder & Hallet 1979; Drewry 1986; Gray 2001). The long, linear and parallel grooves with local ridges exhibited by the flat-lying surface of Bedford Sandstone suggest that these Nye channels formed through the subglacial erosion of a previously striated surface such as is produced by glaciers moving over moderately lithified and unconsolidated sediments (e.g. Beuf *et al*. 1971, figs 37 and 62; Savage 1972; Deynoux 1980; López-Gamundi & Martinez 2000). Such an origin is plausible, because at the time of glaciation the Bedford Sandstone was undeformed and only a few million years old. The lithification of the Bedford Sandstone would have been greatly advanced during subsequent burial by >5 km of Proterozoic sedimentary and volcanic rocks.

### *Sculpted forms*

Erosional features displayed by the unconformity surface, such as sichelwannen, sinuous and strongly curved grooves, isolated ridges, and pot holes, are comparable with sculpted forms (also termed either plastically moulded forms or 'p-forms') ascribed to the erosion of bedrock by subglacial meltwaters (e.g. Shaw 1994; Benn & Evans 1998; Glasser & Nicholson 1998). The sculpted forms exhibited by the Bedford Sandstone are ascribed to erosion by westward-flowing subglacial meltwaters.

The axis of symmetry of sculpted forms is parallel to ice flow (Benn & Evans 1998). Hence, the orientation of the Nye channels and sculpted forms, such as sichelwannen, that are cut in the Bedford Sandstone indicate westward (towards 280°) ice flow. The unconformity surface described here displays the oldest known Nye channels and sculpted forms.

### *Periglacial frost fissures*

The sharp corners of the vertical cracks in the Bedford Sandstone that are filled by sandstone dykes indicate that the gaps opened after the channelled and sculpted sandstone surface had formed. Hence the cracks probably developed following glacial retreat when the area containing the eroded surface of Bedford Sandstone was in a periglacial setting. These sandstone-filled cracks are interpreted as frost fissures (French & Gozdzik 1988; Svensson 1988) that formed through thermal contraction cracking of the uppermost Bedford Sandstone. The cracks, in their dimensions and tendency to form a polygonal pattern in plan, are comparable with Pleistocene sand-filled frost fissures in Poland (French & Gozdzik 1988). The interpretation of periglacial thermal contraction cracking explains why one dyke in the Bedford Sandstone extends upwards into overlying pebbly sandstone; evidently the sand veneering the Bedford Sandstone also underwent such cracking.

The occurrence of frost fissures implies a mean annual air temperature of <0 to <−4 °C and rapid temperature drops (Karte 1983). Recent frost fissuring in Sweden occurred during rapid falls of air temperature between −10 and −20 °C (Svensson 1988).

### *Glaciofluvial deposits*

The conglomerate facies at the base of the King Leopold Sandstone may be compared with glaciofluvial deposits. Features of late Pleistocene glaciofluvial deposits in Québec (Harricana glaciofluvial complex) and Ontario, Canada (Brennand 1994; Brennand & Shaw 1996) that can be matched with features of the conglomerate facies include: tabular, ungraded beds 1–5 m thick of matrix- and clast-supported, bimodal to polymodal gravel, with cobbles and boulders dominant; subrounded to well-rounded clasts; imbricate clusters of larger clasts; medium–coarse, cross-bedded sand; and alternating sand and gravel beds. The matrix-rich gravel indicates rapid deposition from a highly concentrated dispersion (Brennand 1994) and the sand–gravel alternation implies highly unsteady flow (Brennand & Shaw 1996). Poorly sorted, matrix- and clast-supported gravel and conglomerate with subrounded to rounded clasts occur in glaciofluvial deposits elsewhere, such as sandur deposits in Iceland (Maizels 1993) and late Palaeozoic glacial outwash in India (Casshyap & Tewari 1982). The subrounded to well-rounded form of cobbles and boulders in the Harricana complex and other glaciofluvial deposits reflects distance of transport and vigour of flow (Brennand 1994). Clusters of boulders in the conglomerate facies of the King Leopold Sandstone (Fig. 10c) that are aligned along the palaeocurrent direction are comparable in orientation and dimensions with 'cluster bedforms' and 'longitudinal ridges' in alluvial gravels (Brayshaw 1984; Bluck 1987) and glaciofluvial deposits (Brennand 1994; Brennand & Shaw 1996).

The Harricana glaciofluvial complex in Québec (Brennand & Shaw 1996) has a further similarity with the conglomerate facies of the King Leopold Sandstone in being associated with bedrock streamlined erosional features such as grooves and sculpted forms interpreted as the products of subglacial meltwater floods. Brennand & Shaw (1996) viewed the Harricana complex as a subglacial landform. The westward palaeocurrent direction for the conglomerate facies agrees with the orientation of the underlying Nye channels and sculpted forms near Lansdowne and is consistent with a subglacial meltwater origin for this facies.

Accordingly, the conglomerate facies of the King Leopold Sandstone is interpreted as glaciofluvial in origin. The presence of clasts with flatiron shapes and rare striations in the conglomerate facies is consistent with a glacial setting. The apparent absence of diamictite may indicate the glaciofluvial reworking of any older moraines.

Einkanter are the predominant ventifact in the conglomerate facies and are the most common ventifact type in late Pleistocene deposits in NW Saskatchewan, Canada (Fisher 1996). The flutes and pits in several pebbles from the conglomerate facies are like features of ventifacts from Antarctica (Selby 1977) and Late Glacial sites in the Falkland Islands (Clark & Wilson 1992). The presence of rare ventifacts in the conglomerate facies suggests that a periglacial setting marked by either strong localized or katabatic winds (Derbyshire & Owen 1996) followed glacial retreat. The occurrence of ventifacts and frost fissures implies a cold, windy periglacial climate.

The cobbles and boulders of quartzarenite and sandstone in

the conglomerate facies are similar lithologically to the lower Bedford Sandstone of the underlying Speewah Basin (Thorne *et al*. 1999), suggesting extrabasinal derivation. The presence of clasts of vein quartz, metaquartzite, cataclasite, chert and jasper in the conglomerate facies is consistent with extrabasinal derivation from metasedimentary rocks dated at 1880–1840 Ma in the Halls Creek Orogen (Blake *et al*. 1999) to the east of the Kimberley Basin (Fig. 1).

## Discussion

### *Tectonic setting of the King Leopold glaciation*

The northward tilting of the Bedford Sandstone prior to deposition of the King Leopold Sandstone, the change in facies and palaeocurrent directions adjacent to the unconformity between these formations, and the regional extent of the hiatus imply that the unconformity marks an episode of diastrophism that affected the southeastern Kimberley region between 1820 and 1800 Ma. The diastrophism can be ascribed to the Halls Creek Orogeny at 1830–1800 Ma (Tyler & Page 1996), which resulted from the final collision of the Kimberley Craton and the Lucas Craton to the SE (Fig. 11). This event completed the assembly of the North Australian Craton (Myers *et al*. 1996; Tyler *et al*. 1998). The fluvial, upper Bedford Sandstone probably was derived from the rising Halls Creek Orogen to the east. The King Leopold glaciation occurred during the late stage of continental collision near 1800 Ma and evidently was initiated in the elevated Halls Creek Orogen, with glaciers descending westward to near sea level in the southeastern Kimberley region (Fig. 11). The wide extent of the conglomerate facies at the base of the King Leopold Sandstone (Fig. 1) implies the presence of an ice cap rather than a restricted mountain glacier.

A major phase of continental collision in Australia between 1830 and 1760 Ma brought together the North Australian and West Australian cratons (inset, Fig. 1; Cawood & Tyler 2004), and around 1.8 Ga a pre-Rodinia supercontinent, 'Hudsonland' of Pesonen *et al*. (2003) and 'Columbia' of Zhao *et al*. (2002), was assembled. This worldwide diastrophism and associated orogeny, with which the King Leopold glaciation was penecontemporaneous, may have contributed to global cooling (e.g. Worsley *et al*. 1984; Moore & Worsley 1994). In contrast, early Palaeoproterozoic (*c*. 2.3 Ga) glaciation in Canada occurred during breakup of the end-Archaean supercontinent 'Kenorland' (Young *et al*. 2001). Interestingly, late Palaeoproterozoic supercontinental assembly and glaciation in northwestern Australia followed a major episode of Superior-type iron-formation deposition, which has been dated at 1880 ± 2 Ma (Findlay *et al*. 1995) and 1878.3 ± 1.3 Ma (Fralick *et al*. 2002).

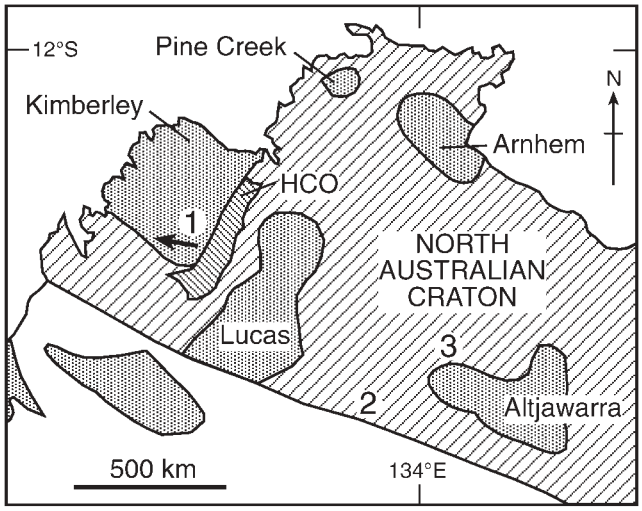


**Fig. 11.** Map of northwestern and central Australia showing Archaean cratons (stippled) within the Proterozoic North Australian Craton (modified from Myers *et al*. 1996). HCO, Halls Creek Orogen, formed by the collision of the Kimberley and Lucas cratons in the late Palaeoproterozoic. The arrow shows the inferred direction of ice flow in the Lansdowne area of the Kimberley Basin (1) during the 1.8 Ga King Leopold glaciation. Transgressive marine successions correlative with the King Leopold Sandstone occur in the Reynolds Range Group (2) and the Hatches Creek Group (3) in central Australia (see text for details).

### *Late Palaeoproterozoic sea-level changes*

A late Palaeoproterozoic fluctuation of sea level is recorded by the sedimentary rocks described here. A relative fall in sea level is implied by the influx of the fluvial upper Bedford Sandstone, and the glaciofluvial deposits at the base of the King Leopold Sandstone are followed conformably by transgressive shallow-marine quartzarenite. Importantly, transgressive shallow-marine successions that are correlative with the King Leopold Sandstone occur in central Australia up to 1000 km east of the Kimberley Basin (Fig. 11). The *c*. 1800 Ma Reynolds Range Group in central Australia commences with a poorly sorted, matrix-supported, polymict conglomerate 1–15 m thick, interpreted as continental lag, that rests unconformably on basement rocks (Dirks 1990; Dirks & Norman 1992). The conglomerate is followed by a quartzarenite facies up to 500 m thick that is interpreted as a transgressive succession deposited on a marine shelf dominated by longshore currents directed southeastwards. Dirks (1990) correlated the Reynolds Range Group with a transgressive, shallow-marine, siliciclastic succession of the *c*. 1800 Ma Hatches Creek Group 350 km to the NE (Blake & Page 1988). He concluded that at 1800 Ma a depositional basin may have covered an extensive area of central and northern Australia.

The occurrence of *c*. 1800 Ma transgressive marine successions in the Kimberley Basin and central Australia suggests that the transgression resulted, in part at least, from glacio-eustatic rise in sea level following the King Leopold glaciation. The preceding relative fall of sea level recorded by the fluvial upper Bedford Sandstone also may have been partly glacio-eustatic. These changes of sea level may be of wider significance and have important implications for late Palaeoproterozoic palaeogeography.

### *Late Palaeoproterozoic climate*

Late Palaeoproterozoic glaciation has been proposed for several continents but none has been verified. Gellatly (1971) interpreted a 'boulder phyllite' in the Halls Creek Orogen as having been deposited by floating ice. The boulder phyllite is directly overlain by the Whitewater Volcanics, which have a U–Pb zircon age of 1855 ± 5 Ma (Page & Sun 1994), hence deposition of the boulder phyllite preceded the King Leopold glaciation by 50–60 million years. A glacial origin has been suggested for poorly sorted conglomerates and diamictite, including the Gangau tilloid, of the Semri Group at the base of the Vindhyan Supergroup in central India (Williams & Schmidt 1996). U–Pb zircon dating of volcanic horizons in the Semri Group has yielded ages

of 1628 ± 8 Ma and 1599 ± 8 Ma (Rasmussen *et al*. 2002) and 1631 ± 5 Ma (Ray *et al*. 2002). Williams & Schmidt (1996) discussed the origin of these purported glaciogenic rocks, concluding that in no case has a glacial origin been demonstrated and arguing that the Gangau Tilloid is a continental debris-flow deposit.

Because of the lack of verified late Palaeoproterozoic–Mesoproterozoic glaciogenic deposits, the concept of a global non-glacial interval *c*. 2200–800 Ma between established early Palaeoproterozoic and late Neoproterozoic glaciations has almost become a paradigm, and a strong atmospheric greenhouse effect has been proposed for that time span (Pavlov *et al*. 2003). However, the implied low palaeolatitude and wide extent of the King Leopold glaciation suggest an extreme climatic event, albeit possibly short-lived, *c*. 1800 Ma. The present finding thus reduces the duration of the apparent non-glacial interval by 400 million years. It is concluded that the claimed non-glacial interval *c*. 2200–800 Ma reflects, at least partly, incomplete knowledge of the late Palaeoproterozoic to early Neoproterozoic stratigraphic record.

The conformable relationship between the glaciofluvial deposits at the base of the King Leopold Sandstone and the overlying shallow-marine succession implies that glaciation in the south-eastern Kimberley Basin occurred near sea level. The present study extends the list of Proterozoic glaciations near sea level in low palaeolatitudes (e.g. Schmidt & Williams 1995; Evans *et al*. 1997; Park 1997; Williams & Schmidt 1997; Evans 2000), thus reinforcing the contrast between Proterozoic glacial distribution and the high to moderate palaeolatitudes of Palaeozoic glaciations (Crowell 1999).

## Conclusions

Linear, parallel grooves and associated erosional features exhibited by an unconformity surface developed on low-dipping, late Palaeoproterozoic sandstone in the Kimberley region, Western Australia, are interpreted as Nye channels and sculpted forms eroded by subglacial meltwaters. An overlying, poorly sorted conglomerate facies up to 15 m thick at the base of the *c*. 1800 Ma King Leopold Sandstone is regarded as glaciofluvial in origin. The Nye channels, sculpted forms and conglomerate facies together record late Palaeoproterozoic continental glaciation in northwestern Australia. The orientation of the Nye channels and sculpted forms and the palaeocurrent direction for the conglomerate facies indicate westward flow of ice. Following glacial retreat, frost fissures formed in the channelled surface in a periglacial setting. Rare ventifacts in the conglomerate facies indicate strong periglacial winds. The glaciofluvial deposits are conformably overlain by quartzarenite of probable shallow-marine origin, implying that glaciation reached close to sea level.

The King Leopold glaciation evidently was initiated in the Halls Creek Orogen to the east towards the close of the 1830–1800 Ma Halls Creek Orogeny, which marked final amalgamation of the North Australian Craton. Worldwide supercontinental assembly was completed around 1800 Ma and may have contributed to global cooling. Glaciation in the Kimberley Basin was coeval with marine regression and was followed by transgression at *c*. 1800 Ma, which also affected late Palaeoproterozoic basins in central Australia. These late Palaeoproterozoic changes of sea level may have been partly glacio-eustatic.

Palaeomagnetic data for late Palaeoproterozoic rocks in the Kimberley region, and the Australian Precambrian apparent polar wander path, imply that the King Leopold glaciation occurred in low palaeolatitudes (<20°). Hence the enigma of glaciation near sea level in low palaeolatitudes, which marks the early Palaeoproterozoic and late Neoproterozoic, applies also to the late Palaeoproterozoic. Recognition of the King Leopold glaciation reduces the duration of the alleged global non-glacial interval between *c*. 2200 and 800 Ma by 400 million years, and indicates that the claimed absence of glaciation during this interval reflects, in part at least, incomplete knowledge of the Proterozoic stratigraphic record.

I thank R. Close, W. Hewitt, B. Mills and K. Slee for assistance with field work in 1969. J. Harms and the late H. Steiner provided helpful discussions during field work in 1976 and 1977. T. Williams assisted with the preparation of the figures, and M. Hambrey, J. Macquaker and P. Eriksson provided constructive reviews. The work was supported by The Broken Hill Pty. Co. Ltd. and a Professorial Fellowship of the Australian Research Council.

## References

Abbott, S.T. & Sweet, I.P. 2000. Tectonic control on third-order sequences in a siliciclastic ramp-style basin: an example from the Roper Superbasin (Mesoproterozoic), northern Australia. *Australian Journal of Earth Sciences*, **47**, 637–657.

Benn, D.I. & Evans, D.J.A. 1998. *Glaciers and Glaciation*. Arnold, London.

Bennett, R., Page, R.W. & Bladon, G.M. 1975. *Catalogue of Isotopic Age Determinations on Australian Rocks, 1966–70*. Bureau of Mineral Resources, Geology and Geophysics, Canberra, Report, **162**.

Beuf, S., Biju-Duval, B., de Charpal, O., Rognon, P., Gariel, O. & Bennacef, A. 1971. *Les Grès du Paléozoïque Inférieur au Sahara*. Publications de l'Institut Français du Pétrole. Collection 'Science et Technique du Pétrole', Technip, Paris, **18**.

Blake, D.H. & Page, R.W. 1988. The Proterozoic Davenport province, central Australia: regional geology and geochronology. *Precambrian Research*, **40–41**, 329–340.

Blake, D.H., Stewart, A.J., Sweet, I.P. & Hone, I.G. 1987. *Geology of the Proterozoic Davenport Province, Central Australia*. Bureau of Mineral Resources, Geology and Geophysics, Canberra, Bulletin, **226**.

Blake, D.H., Tyler, I.M., Griffin, T.J., Sheppard, S., Thorne, A.M. & Warren, R.G. 1999. *Geology of the Halls Creek 1:100 000 Sheet Area (4461), Western Australia*. Australian Geological Survey Organisation, Canberra.

Bluck, B.J. 1987. Bed forms and clast size changes in gravel-bed rivers. *In:* Richards, K. (ed.) *River Channels. Environment and Process*. Blackwell, Oxford, 159–178.

Brayshaw, A.C. 1984. Characteristics and origin of cluster bedforms in coarse-grained alluvial channels. *In:* Koster, E.H. & Steel, R.J. (eds) *Sedimentology of Gravels and Conglomerates*. Canadian Society of Petroleum Geologists Memoir, **10**, 77–85.

Brennand, T.A. 1994. Macroforms, large bedforms and rhythmic sedimentary sequences in subglacial eskers, south–central Ontario: implications for esker genesis and meltwater regime. *Sedimentary Geology*, **91**, 9–55.

Brennand, T.A. & Shaw, J. 1996. The Harricana glaciofluvial complex, Abitibi region, Quebec: its genesis and implications for meltwater regime and ice-sheet dynamics. *Sedimentary Geology*, **102**, 221–262.

Carter, J.D. 1976. Recent exploration for uranium in the Kimberley region. *Geological Survey of Western Australia Annual Report*, 1975, 95–108.

Casshyap, S.M. & Tewari, R.C. 1982. Facies analysis and paleogeographic implications of a late Paleozoic glacial outwash deposit Bihar, India. *Journal of Sedimentary Petrology*, **52**, 1243–1256.

Cawood, P.A. & Tyler, I.M. 2004. Assembling and reactivating the Proterozoic Capricorn Orogen: lithotectonic elements, orogenies, and significance. *Precambrian Research*, **128**, 201–218.

Clark, R. & Wilson, P. 1992. Occurrence and significance of ventifacts in the Falkland Islands, South Atlantic. *Geografiska Annaler*, **74A**, 35–46.

Crowell, J.C. 1999. *Pre-Mesozoic Ice Ages: their Bearing on Understanding the Climate System*. Geological Society of America, Memoir, **192**.

Derbyshire, E. & Owen, L.A. 1996. Glacioaeolian processes, sediments and landforms. *In:* Menzies, J. (ed.) *Glacial Environments 2, Past Glacial Environments—Sediments, Forms and Techniques*. Heinemann, Oxford, 213–237.

Derrick, G.M., Gellatly, D.C. & Mikolajczak, A.S. 1965. *Lansdowne, W.A. Sheet SE 52-5*. Bureau of Mineral Resources, Geology and Geophysics, Canberra, and Geological Survey of Western Australia 1:250 000 Geological Series.

Deynoux, M. 1980. *Les Formations Glaciaires du Précambrien Terminal et du la*

*Fin de l'Ordovicien en Afrique de l'Ouest*. Travaux des Laboratoires des Sciences de la Terre St Jérome, Marseille, **17**.

Dirks, P.H.G.M. 1990. Intertidal and subtidal sedimentation during a mid-Proterozoic marine transgression, Reynolds Range Group, Arunta Block, central Australia. *Australian Journal of Earth Sciences*, **37**, 409–422.

Dirks, P.H.G.M. & Norman, A.R. 1992. Physical sedimentation processes on a mid-Proterozoic (1800 Ma) shelf: the Reynolds Range Group, Arunta Block, central Australia. *Precambrian Research*, **59**, 225–241.

Drewry, D. 1986. *Glacial Geologic Processes*. Edward Arnold, London.

Eriksson, P.G., Condie, K.C. & Tirsgaard, H. *et al.* 1998. Precambrian clastic sedimentation systems. *Sedimentary Geology*, **120**, 5–53.

Evans, D.A.D. 2000. Stratigraphic, geochronological, and paleomagnetic constraints upon the Neoproterozoic climatic paradox. *American Journal of Science*, **300**, 347–433.

Evans, D.A., Beukes, N.J. & Kirschvink, J.L. 1997. Low-latitude glaciation in the Palaeoproterozoic era. *Nature*, **386**, 262–266.

Eyles, N. 1993. Earth's glacial record and its tectonic setting. *Earth-Science Reviews*, **35**, 1–248.

Eyles, N. & Boyce, J.I. 1998. Kinematic indicators in fault gouge: tectonic analog for soft-bedded ice sheets. *Sedimentary Geology*, **116**, 1–12.

Findlay, J.M., Parrish, R.R., Birkett, T.C. & Watanabe, D.H. 1995. U–Pb ages from the Nimish Formation and Montagnais glomeroporphyritic gabbro of the central New Québec Orogen, Canada. *Canadian Journal of Earth Sciences*, **32**, 1208–1220.

Fisher, T.G. 1996. Sand-wedge and ventifact palaeoenvironmental indicators in north-west Saskatchewan, Canada, 11 ka to 9.9 ka BP. *Permafrost and Periglacial Processes*, **7**, 391–408.

Fralick, P., Davis, D.W. & Kissin, S.A. 2002. The age of the Gunflint Formation, Ontario, Canada: single zircon U–Pb age determinations from reworked volcanic ash. *Canadian Journal of Earth Sciences*, **39**, 1085–1091.

French, H.M. & Gozdzik, J.S. 1988. Pleistocene epigenetic and syngenetic frost fissures, Belchatów, Poland. *Canadian Journal of Earth Sciences*, **25**, 2017–2027.

Gellatly, D.C. 1971. Possible Archaean rocks of the Kimberley region, Western Australia. *In:* Glover, J.E. (ed.) *Symposium on Archaean Rocks*. Geological Society of Australia Special Publication, **3**, 93–101.

Gellatly, D.C., Derrick, G.M. & Plumb, K.A. 1970. Proterozoic palaeocurrent directions in the Kimberley region, northwestern Australia. *Geological Magazine*, **107**, 249–257.

Gellatly, D.C., Derrick, G.M. & Plumb, K.A. 1975. *The Geology of the Lansdowne 1:250 000 Sheet Area, Western Australia*. Bureau of Mineral Resources, Geology and Geophysics, Canberra, Report, **152**.

Glasser, N.F. & Nicholson, F.H. 1998. Subglacial meltwater erosion at Loch Treig. *Scottish Journal of Geology*, **34**, 7–13.

Gray, H.H. 2001. Subglacial meltwater channels (Nye channels or N-channels) in sandstone at Hindostan Falls, Martin County, Indiana. *Proceedings of the Indiana Academy of Science*, **110**, 1–8.

Griffin, T.J. & Grey, K. 1990a. King Leopold and Halls Creek orogens. *In: Geology and Mineral Resources of Western Australia*. Geological Survey of Western Australia Memoir, **3**, 232–255.

Griffin, T.J. & Grey, K. 1990b. Kimberley Basin. *In: Geology and Mineral Resources of Western Australia*. Geological Survey of Western Australia Memoir, **3**, 293–304.

Griffin, T.J., Tyler, I.M. & Playford, P.E. 1993. *Lennard River, W.A., 3rd edition*. Geological Survey of Western Australia 1:250 000 Geological Series Explanatory Notes.

Hughes, F.E. & Harms, J.E. 1975. Radioactive King Leopold conglomerate. *In:* Knight, C.L. (ed.) *Economic Geology of Australia and Papua New Guinea. 1. Metals*. Australasian Institute of Mining and Metallurgy Monograph, **5**, 257–259.

Idnurm, M., Giddings, J.W. & Plumb, K.A. 1995. Apparent polar wander and reversal stratigraphy of the Palaeo–Mesoproterozoic southeastern McArthur Basin, Australia. *Precambrian Research*, **72**, 1–41.

Karte, J. 1983. Periglacial phenomena and their significance as climatic and edaphic indicators. *GeoJournal*, **7**, 329–340.

Li, Z.X. 2000. Palaeomagnetic evidence for unification of the North and West Australian cratons by *ca*. 1.7 Ga: new results from the Kimberley Basin of northwestern Australia. *Geophysical Journal International*, **142**, 173–180.

López-Gamundi, O. & Martinez, M. 2000. Evidence of glacial abrasion in the Calingasta–Uspallata and western Paganzo basins, mid-Carboniferous of western Argentina. *Palaeogeography, Palaeoclimatology, Palaeoecology*, **159**, 145–165.

Maizels, J. 1993. Lithofacies variations within sandur deposits: the role of runoff regime, flow dynamics and sediment supply characteristics. *Sedimentary Geology*, **85**, 299–325.

McElhinny, M.W. & Evans, M.E. 1976. Palaeomagnetic results from the Hart Dolerite of the Kimberley Block, Australia. *Precambrian Research*, **3**, 231–241.

McNaughton, N.J., Rasmussen, B. & Fletcher, I.R. 1999. SHRIMP uranium–lead dating of xenotime in siliciclastic sedimentary rocks. *Science*, **285**, 78–80.

Miall, A.D. 1996. *The Geology of Fluvial Deposits*. Springer, Berlin.

Moncrieff, A.C.M. & Hambrey, M.J. 1988. Late Precambrian glacially-related grooved and striated surfaces in the Tillite Group of Central East Greenland. *Palaeogeography, Palaeoclimatology, Palaeoecology*, **65**, 183–200.

Moore, T.L. & Worsley, T.R. 1994. Orogenic enhancement of weathering and continental ice-sheet initiation. *In:* Klein, G.D. (ed.) *Pangea: Paleoclimate, Tectonics, and Sedimentation During Accretion, Zenith, and Breakup of a Supercontinent*. Geological Society of America, Special Paper, **288**, 75–89.

Myers, J.S., Shaw, R.D. & Tyler, I.M. 1996. Tectonic evolution of Proterozoic Australia. *Tectonics*, **15**, 1431–1446.

Ozchron 2004. Ozchron National Geochronology database. Geoscience Australia, Canberra. http://www.ga.gov.au/oracle/ozchron/TOC.jsp.

Page, R. & Sun, S.-S. 1994. Evolution of the Kimberley region, W.A. and adjacent Proterozoic inliers—new geochronological constraints. *Geological Society of Australia Abstracts*, **37**, 332–333.

Park, J.K. 1997. Paleomagnetic evidence for low-latitude glaciation during deposition of the Neoproterozoic Rapitan Group, Mackenzie Mountains, N.W.T., Canada. *Canadian Journal of Earth Sciences*, **34**, 34–49.

Pavlov, A.A., Hurtgen, M.T., Kasting, J.F. & Arthur, M.A. 2003. Methane-rich Proterozoic atmosphere? *Geology*, **31**, 87–90.

Pesonen, L.J., Elming, S.-Å. & Mertanen, S. *et al.* 2003. Palaeomagnetic configuration of continents during the Proterozoic. *Tectonophysics*, **375**, 289–324.

Pettijohn, F.J. 1975. *Sedimentary Rocks*, *3rd*. Harper & Row, New York.

Plumb, K.A. 1968. *Lissadell, Western Australia, Sheet SE/52-2*. Bureau of Mineral Resources, Geology and Geophysics, Canberra, 1:250 000 Geological Series Explanatory Notes.

Plumb, K.A. & Gemuts, I. 1976. *Precambrian Geology of the Kimberley Region, Western Australia*. 25th International Geological Congress, Sydney, Excursion Guide, **44C**.

Plumb, K.A., Ahmad, M. & Wygralak, A.S. 1990. Mid-Proterozoic basins of the North Australian Craton—regional geology and mineralisation. *In:* Hughes, F.E. (ed.) *Geology of the Mineral Deposits of Australia and Papua New Guinea, Volume 1*. Australasian Institute of Mining and Metallurgy Monograph, **14**, 881–902.

Potter, P.E. & Pettijohn, F.J. 1977. *Paleocurrents and Basin Analysis*, *2nd*. Springer, Berlin.

Rasmussen, B., Bose, P.K., Sarkar, S., Banerjee, S., Fletcher, I.R. & McNaughton, N.J. 2002. 1.6 Ga U–Pb zircon age for the Chorhat Sandstone, lower Vindhyan, India: possible implications for early evolution of animals. *Geology*, **30**, 103–106.

Ray, J.S., Martin, M.W., Veizer, J. & Bowring, S.A. 2002. U–Pb zircon dating and Sr isotope systematics of the Vindhyan Supergroup, India. *Geology*, **30**, 131–134.

Savage, N.M. 1972. Soft-sediment glacial grooving of Dwyka age in South Africa. *Journal of Sedimentary Petrology*, **42**, 307–308.

Schmidt, P.W. & Clark, D.A. 1994. Palaeomagnetism and magnetic anisotropy of Proterozoic banded-iron formations and iron ores of the Hamersley Basin, Western Australia. *Precambrian Research*, **69**, 133–155.

Schmidt, P.W. & Williams, G.E. 1995. The Neoproterozoic climatic paradox: equatorial palaeolatitude for Marinoan glaciation near sea level in South Australia. *Earth and Planetary Science Letters*, **134**, 107–124.

Selby, M.J. 1977. Transverse erosional marks on ventifacts from Antarctica. *New Zealand Journal of Geology and Geophysics*, **20**, 949–969.

Sharp, M., Gemmell, J.C. & Tison, J.-L. 1989. Structure and stability of the former subglacial drainage system of the Glacier de Tsanfleuron, Switzerland. *Earth Surface Processes and Landforms*, **14**, 119–134.

Shaw, J. 1994. Hairpin erosional marks, horseshoe vortices and subglacial erosion. *Sedimentary Geology*, **91**, 269–283.

Sheppard, S., Tyler, I.M. & Hoatson, D.M. 1997. *Geology of the Mount Remarkable 1:100 000 Sheet*. Geological Survey of Western Australia 1:100 000 Geological Series Explanatory Notes.

Sheppard, S., Tyler, I.M., Griffin, T.J. & Taylor, W.R. 1999. Palaeoproterozoic subduction-related and passive margin basalts in the Halls Creek Orogen, northwest Australia. *Australian Journal of Earth Sciences*, **46**, 679–690.

Svensson, H. 1988. Recent frost fissuring in a coastal area of southwestern Sweden. *Norsk Geografisk Tidsskrift*, **42**, 271–277.

Thorne, A.M., Sheppard, S. & Tyler, I.M. 1999. *Lissadell, W.A., 2nd*. Geological Survey of Western Australia 1:250 000 Geological Series Explanatory Notes.

Tyler, I.M. & Griffin, T.J. 1990. Structural development of the King Leopold Orogen, Kimberley region, Western Australia. *Journal of Structural Geology*, **12**, 703–714.

Tyler, I.M. & Page, R.W. 1996. Palaeoproterozoic deformation, metamorphism and igneous intrusion in the central zone of the Lamboo Complex, Halls Creek Orogen. *Geological Society of Australia Abstracts*, **41**, 450.

Tyler, I.M., Pirajno, F., Bagas, L., Myers, J.S. & Preston, W.A. 1998. The geology and mineral deposits of the Proterozoic in Western Australia. *AGSO (Australian Geological Survey Organisation) Journal of Australian Geology and Geophysics*, **17**, 223–244.

Walder, J. & Hallet, B. 1979. Geometry of former subglacial water channels and cavities. *Journal of Glaciology*, **23**, 335–346.

Williams, G.E. 1969. *Stratigraphy and sedimentation in the Mount Bedford area, W.A*. Report to The Broken Hill Proprietary Company Limited, Melbourne.

Williams, G.E. & Schmidt, P.W. 1996. Origin and palaeomagnetism of the Mesoproterozoic Gangau tilloid (basal Vindhyan Supergroup), central India. *Precambrian Research*, **79**, 307–325.

Williams, G.E. & Schmidt, P.W. 1997. Paleomagnetism of the Paleoproterozoic Gowganda and Lorrain formations, Ontario: low paleolatitude for Huronian glaciation. *Earth and Planetary Science Letters*, **153**, 157–169.

Williams, G.E., Schmidt, P.W. & Clark, D.A. 2004. Palaeomagnetism of iron-formation from the late Palaeoproterozoic Frere Formation, Earaheedy Basin, Western Australia: palaeogeographic and tectonic implications. *Precambrian Research*, **128**, 367–383.

Worsley, T.R., Nance, D. & Moody, J.B. 1984. Global tectonics and eustacy for the past 2 billion years. *Marine Geology*, **58**, 373–400.

Young, G.M., Long, D.G.F., Fedo, C.M. & Nesbitt, H.W. 2001. Paleoproterozoic Huronian basin: product of a Wilson cycle punctuated by glaciations and a meteorite impact. *Sedimentary Geology*, **141–142**, 233–254.

Zhao, G., Cawood, P.A., Wilde, S.A. & Sun, M. 2002. Review of global 2.1–1.8 Ga orogens: implications for a pre-Rodinia supercontinent. *Earth-Science Reviews*, **59**, 125–162.

Received 10 October 2003; revised typescript accepted 14 May 2004.
Scientific editing by Joe Macquaker